AFRL-DE-TR-
1999-1036

The Ferratron: A High-Voltage, High Rep-Rate, Low Jitter, Ultrawideband Switch With A Ferroelectric Trigger

Leland H. Bowen et al.

Farr Research, Inc.
614 Paseo Del Mar NE
Albuquerque, NM 87123

February 1999

Final Report

AIR FORCE RESEARCH LABORATORY
Directed Energy Directorate
3550 Aberdeen Ave SE
AIR FORCE MATERIEL COMMAND
KIRTLAND AIR FORCE BASE, NM 87117-5776

AFRL-DE-TR-1999-1036

Using Government drawings, specifications, or other data included in this document for any purpose other than Government procurement does not in any way obligate the U.S. Government. The fact that the Government formulated or supplied the drawings, specifications, or other data, does not license the holder or any other person or corporation; or convey any rights or permission to manufacture, use, or sell any patented invention that may relate to them.

This report has been reviewed by the Public Affairs Office and is releasable to the National Technical Information Service (NTIS). At NTIS, it will be available to the general public, including foreign nationals.

If you change your address, wish to be removed from this mailing list, or your organization no longer employs the addressee, please notify AFRL/DEHP, 3550 Aberdeen Ave SE, Kirtland AFB, NM 87117-5776.

Do not return copies of this report unless contractual obligations or notice on a specific document requires its return.

This report has been approved for publication.

Dr Jane Lehr, DR-II
Project Manager

FOR THE COMMANDER

MARK FRANZ, Lt Col, USAF
Chief, High Power Microwave Division

R. EARL GOOD, SES
Director, Directed Energy

REPORT DOCUMENTATION PAGE

Form Approved
OMB No. 074-0188

1. AGENCY USE ONLY (Leave blank)	2. REPORT DATE	3. REPORT TYPE AND DATES COVERED
	February 1999	Final Report, May 98 – Jan 1999

4. TITLE AND SUBTITLE
The Ferratron: A High-Voltage, High Rep-Rate, Low Jitter, Ultra-Wideband Switch With A Ferroelectric Trigger

5. FUNDING NUMBERS
C: F29601-98-C-0150
PE: 65502F
PR: 3005
TA: DO
WU:AA

6. AUTHOR(S)
Leland H. Bowen, Everett G. Farr, Juan M. Elizondo, and Jane Lehr *

7. PERFORMING ORGANIZATION NAME(S) AND ADDRESS(ES)
Farr Research, Inc.
614 Paseo Del Mar NE
Albuquerque, NM 87123

8. PERFORMING ORGANIZATION REPORT NUMBER

9. SPONSORING / MONITORING AGENCY NAME(S) AND ADDRESS(ES)
Air Force Research Laboratory / Directed Energy
3550 Aberdeen Ave SE
Kirtland AFB, NM 87117-5776

10. SPONSORING / MONITORING AGENCY REPORT NUMBER
AFRL-DE-TR-1999-1036

11. SUPPLEMENTARY NOTES

12a. DISTRIBUTION / AVAILABILITY STATEMENT
Approved for Public Release; Distribution is Unlimited.

12b. DISTRIBUTION CODE

13. ABSTRACT ***(Maximum 200 Words)***

The system is a novel application of ferroelectric ceramics combined with a gas flow scheme that provides reliable triggering at high repetition rates. The design can be interpreted as an active trigatron-like switch where the ferroelectric ceramic behaves as an electron/corona source and the trigger configuration is that of a simple trigatron with the advantage that the trigger voltages are not as high as the gap voltage.

The trigger system is integrated into a fast gas flow switch chamber design capable of sustaining 500 kV at a pressure of 1500 psi. The switch chamber is tailored to reduce field stress and provide a low inductance current path with a very compact geometry. The high gas flow allows the replacement of the gas in the discharge region on a time scale necessary to sustain the required repetition rate (100 Hz to 1 kHz).

The switch has been successfully operated during the preliminary tests using N_2 at low pressure. The jitter was found to be < 70 Ps at a repetition rate of 1 Hz. The rise time was on the order of 500 Ps. Higher repetition rates, faster rise times, and higher voltages will be attained as testing and development continue.

14. SUBJECT TERMS
Ferratron, Ultra-Wideband, Pulser, Ferroelectric, Trigger, Ceramic, High-Voltage, Low-Jitter, High Rep Rate, Gass Switch

15. NUMBER OF PAGES
26

16. PRICE CODE

17. SECURITY CLASSIFICATION OF REPORT	18. SECURITY CLASSIFICATION OF THIS PAGE	19. SECURITY CLASSIFICATION OF ABSTRACT	20. LIMITATION OF ABSTRACT
UNCLASSIFIED	UNCLASSIFIED	UNCLASSIFIED	UNLIMITED

NSN 7540-01-280-5500

Standard Form 298 (Rev. 2-89)
Prescribed by ANSI Std. Z39-18
298-102

Table of Contents

List of Figures

I. Introduction

High-voltage triggering technology for high repetition rate applications has not kept pace with impressive developments in Ultra Wide Band (UWB) source technology. Unique applications that require a sequential, simultaneous, or delayed source triggering, all at high repetition rates, have not been explored due to the lack of such triggering capabilities. Triggering of UWB and NB sources, especially at high repetition rates, will open a number of system configurations not previously possible.

High-voltage switch triggering has always been implemented by a brute-force approach (overvolted center plane) or an expensive laser triggered gap. The problem is compounded by the typically high gas pressures required to hold off the voltage across the switch and to provide the required rise time. Simple techniques such as trigatron type switches are limited by the high electric field required across the gap and the implicit jitter due to local field variations during high repetition rate operation. Most existing trigger systems originate from work performed during the early 1960's and laser systems developed for Hermes III at Sandia in the early 1980's.

The high-pressure switch being developed by the Farr Research team is based on a novel application of ferroelectric ceramics combined with a gas flow scheme that provides reliable triggering and high repetition rates. We expect this combination to provide solutions to many of the switching problems discussed above. A brief explanation of ferroelectric materials can be found in reference [1]. Ferroelectric ceramic technology has developed electron emitters which can act as fast repetitive trigger sources since they can be operated at repetition rates above 1 MHz [2,3]. The concept is similar to that used for RF-driven atmospheric discharges or so called silent discharges [4].

The system design can be interpreted as an active trigatron-like switch, where the ferroelectric ceramic behaves as an electron/corona source and the trigger configuration is that of a simple trigatron. Since the trigger ceramic pin operates at its own potential, independent from the typical trigatron requirements of electric field and polarization, the trigger voltages are not as high as the gap voltage. The operation of the ferroelectric ceramic trigger system consists of two or three basic steps. First the trigger pulse causes electrons with energies ranging from 5 to 15 eV to be emitted from the surface of the ferroelectric ceramic. These electrons ionize the gas molecules. The ionized gas molecules thus formed are moved downstream to the high field gap causing breakdown and switch operation.

The trigger system is integrated into a fast gas flow switch chamber design, which is capable of sustaining 500 kV and 1500 psig. The switch has fast gas flow to allow gas refreshing between shots or shot bursts. The switch chamber is tailored to reduce field stresses with a very compact geometry. The geometry is such that electric fields are controlled to provide a low inductance current path and a high velocity gas flow. The gas flow allows the replacement of the gas at the discharge region, in the time scale necessary to sustain the required repetition rate (100 Hz to 1 kHz). For the preliminary tests described here dry air and N_2 were used. However, other gasses such as SF_6 or hydrogen can be used.

II. Theory

The switch technology described here is a very innovative use of different discharge schemes. The use of ferroelectric electron emitters as trigger bars and their integration in high-pressure gas discharges opens the possibility for very compact inexpensive and reliable trigger systems.

The magnitude of the induced free charge current density, due to the polarization flipping, is explained by the fact that the magnitude of the polarization vector is:

$$\left|\vec{P}\right| = \sigma_f + \sigma_b \tag{1}$$

where σ_f is the free surface charge and σ_b is the bound charge. Using the vector representation in Figure 2.1, where $\vec{n}$ is the unit vector normal to the surface area and θ is the angle between the polarization vector direction and the unit vector $\vec{n}$, we have

$$\sigma_b = \vec{P} \cdot \vec{n} \tag{2}$$

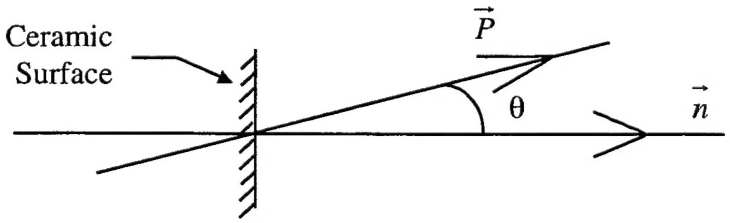

Figure 2.1. Polarization Vector

This yields, after substitution into Equation 1:

$$\sigma_f = \left|\vec{P}\right|(1 - \cos\theta) \tag{3}$$

By definition, the current density (J_f) is:

$$J_f = \frac{d\sigma_f}{dt} = P \sin\theta \frac{d\theta}{dt} \tag{4}$$

For a material such as lead-titanate-zirconate piezo ceramic (LTZ-2) with ε_R = 1,900 [5] and with the expected maximum current for 10 ns polarization flipping time, we have

$$J_f = \frac{d\sigma_f}{dt} = \frac{\Delta P}{\Delta t} = \frac{\varepsilon_o(\varepsilon_R - 1)E_p}{\Delta t}, \qquad J_f = 336 \text{ A / cm}^2 \tag{5}$$

where ε_R is the relative permittivity, $\varepsilon_0 = 8.85\times10^{-12}$ F/m, and the external electric poling field, E_P, is 20 kV/cm. This calculation shows the maximum current possible. Even if we assume 10% extraction efficiency, it still results in a current density of more than 30 A/cm^2 [6].

The trigger mechanism is based on the emission of electrons by the ferroelectric ceramic. A radical difference between this system and conventional technologies is the magnitude of the voltage (or electric field) required to trigger the gap. The ferroelectric based system operates by injecting electrons from the surface of the ceramic into the gas, and then allowing them to avalanche. Other systems basically initiate an avalanche by over-volting the gap, or by pumping photons to create photo-electrons, thus initiating the avalanche.

The production of surface electrons emitted from a ferroelectric material is based on flipping the polarization vector by external means. There is a conduction current that can be established by such a mechanism. The polarization-induced charge (free and bound) is the result of using materials with a high dielectric constant (high electric dipole density), which are permanently "poled." The poling process involves the application of a high external electric field (tens of kV/cm) while the material is under a heating/cooling cycle.

The general electron expulsion scheme can be explained by the following sequence of events. There are only two kinds of electronic charges at the ceramic/gas interface: free charges and bound charges. These charges relate to the emission process as follows:

a) Initially, the ceramic is polarized in a preferred direction. This results in negative bound charges on one surface and positive bound charges on the opposite surface. These charges are neutralized by dust, etc., so no effective electric field is present.

b) The external power supply is connected so that negative voltage is applied to the ceramic surface where negative bound charge is present.

c) When negative voltage is applied (to the negative bound charged surface) the negative bound charges are repelled. The repulsion causes the polarization vector to flip.

d) As long as the negative voltage is applied, negative free charges are deposited, attracted by the already flipping, positive bound charges. Surface conductivity changes by the Poole-Frenkel Effect [7].

$$\sigma(E) = \sigma_o \exp\left[\left(\frac{q^3 E}{\varepsilon_o \varepsilon_R}\right)^{1/2} \Big/ kT\right] \tag{6}$$

where $\sigma(E)$ is the electric field (E) dependent surface conductivity, σ_o is the surface conductivity, q is the electron charge, ε_R is the relative dielectric constant, k is the Boltzman constant, and T is the temperature.

e) When the negative external voltage is removed, the polarization vector flips back. This places the negative bound charges at the same interface as the negative free charges.

f) Fields in the GV/cm range are generated between the free and bound charges. This results in the free charge's violent expulsion from the ceramic's surface.

g) The ceramic returns to its original state.

The preceding description resolves several issues. First, the charges expelled from the surface are free charges, i.e. free electrons with no ions. Second, the electrons (free charges) are deposited by the external power supply. Third, there is no explosive emission, since no bound

charges are being expelled. Last, long pulses are possible by controlling the polarization density and the ceramic's relaxation time.

Note that the current pulse is obtained at the end of the externally applied voltage. This has been observed in most experiments [8]. Also note that relaxation returns the polarization vector to its original state. This may be enhanced by the shape of the hysteresis curve. If the material behaves as a normal ferroelectric, the ideal hysteresis curve is narrowed at the center to allow for a large $\Delta P/\Delta E$. Electron emission is enhanced by high electric fields ($E_{external} >> E_p$) when the material is made with this feature. A second alternative is that the material is anti-ferroelectric and the hysteresis curve is off axis. This means that the external electric field needs to reach an initial value before electron emission is observed. This effect has been observed in the form of enhanced emission after the external electric field is increased beyond the value of the ceramic poling field.

Finally, we note that the poling field is the field which is present during the formation of the ceramic. To be effective as a trigger, the ferroelectric material must be excited by a trigger voltage that creates a field which exceeds the poling field. Only then will the ferroelectric material expel a sufficient number of electrons to trigger a breakdown.

III. High-Voltage, High-Pressure Switch Design

The switch design has a high-strength insulating shell to support the hemispherical electrodes at the desired spacing and to contain the high-pressure gas. The general arrangement of the switch electrodes and the internal ferroelectric trigger are shown in Figures 3.1 – 3.4. The low voltage (grounded) electrode has a hollow center for insertion of the ferroelectric trigger. Multiple (6) ports in the base allow gas flow around the ferroelectric into the gap chamber. The gas then exits through ports in the high voltage electrode. A clear plastic sight tube is provided in the wall of the insulating shell and the outer aluminum ring for visual observation of the arc and for the possible use of a photo-diode detector.

The switch operation relies on the flow of gas ionized by the ferroelectric ceramic. The ferroelectric tip ionizes the gas inside the ionization chamber prior to the main gap. The gas flow moves the ionized material into the gap where avalanche occurs, causing switch closure. Ionization takes place not by a flashover or spark action between the electrode and ground, but by the electron emission by the ferroelectric material producing ionization of the host gas. This process depends upon the appropriate design of the ferroelectric tip, the gas velocity, and gap spacing in relation to the gas recombination rates. This design depends strongly on dn_e/dt rather than dV/dt as is the case in other technologies.

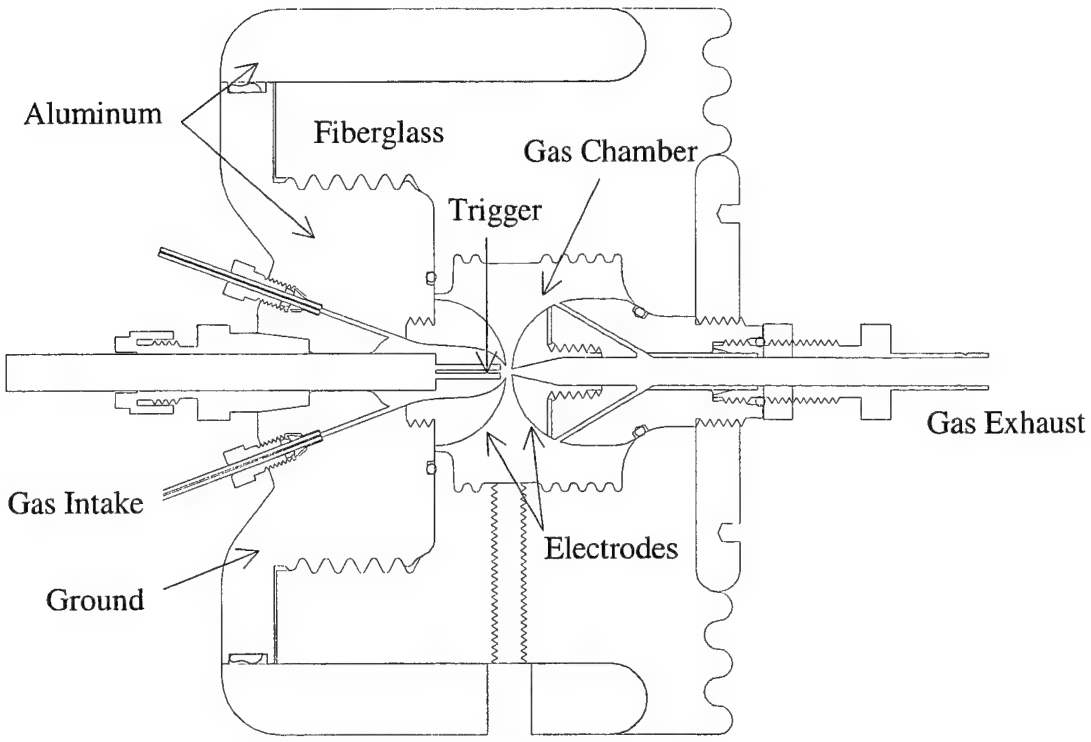

Figure 3.1. Cross-section of switch showing electrode and trigger design. The outer diameter is five inches.

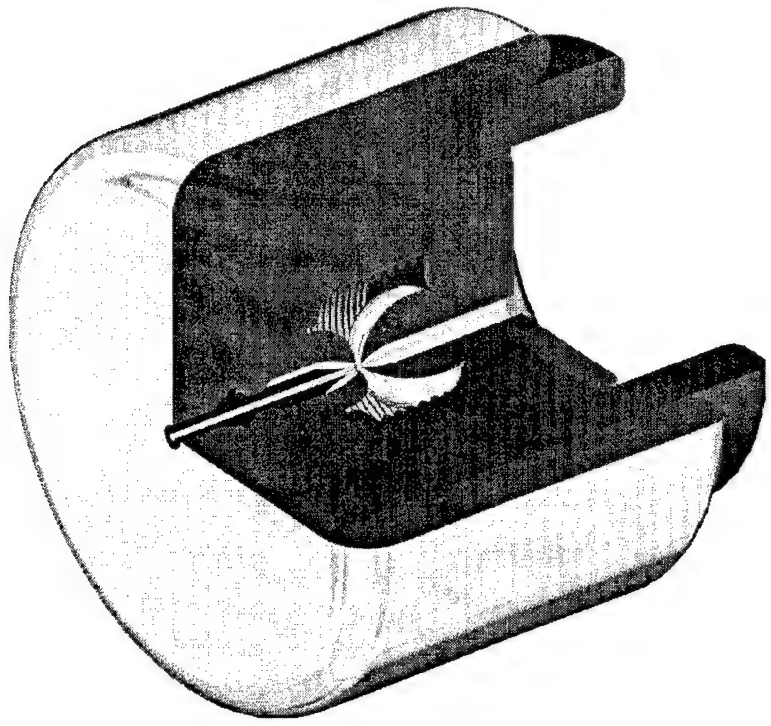

Figure 3.2. Cutaway of the switch (Preliminary Design without Multiple Gas Ports).

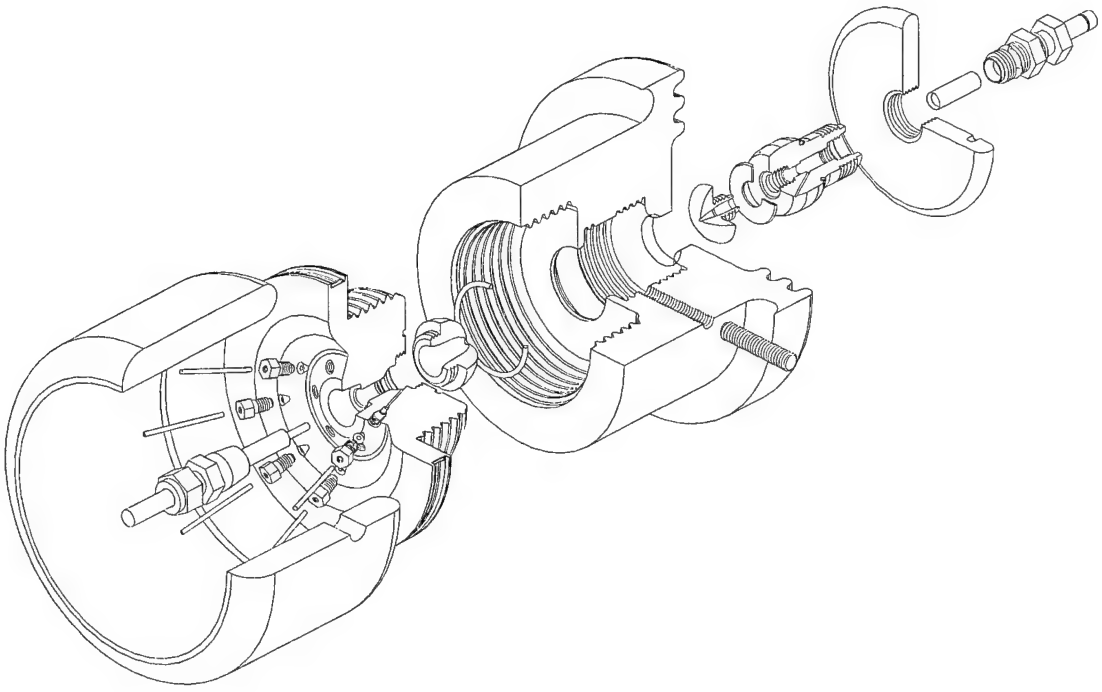

Figure 3.3. Cutaway exploded view of switch showing the electrode and trigger set up. The gas feed lines and insulator, with the high-voltage feed to the ferroelectric tip, are shown on the left. The center section is the insulator which forms the high-pressure gas flow cavity and supports the grounded electrode (left side) and the high-voltage electrode (right side). The gas flow path is from left to right.

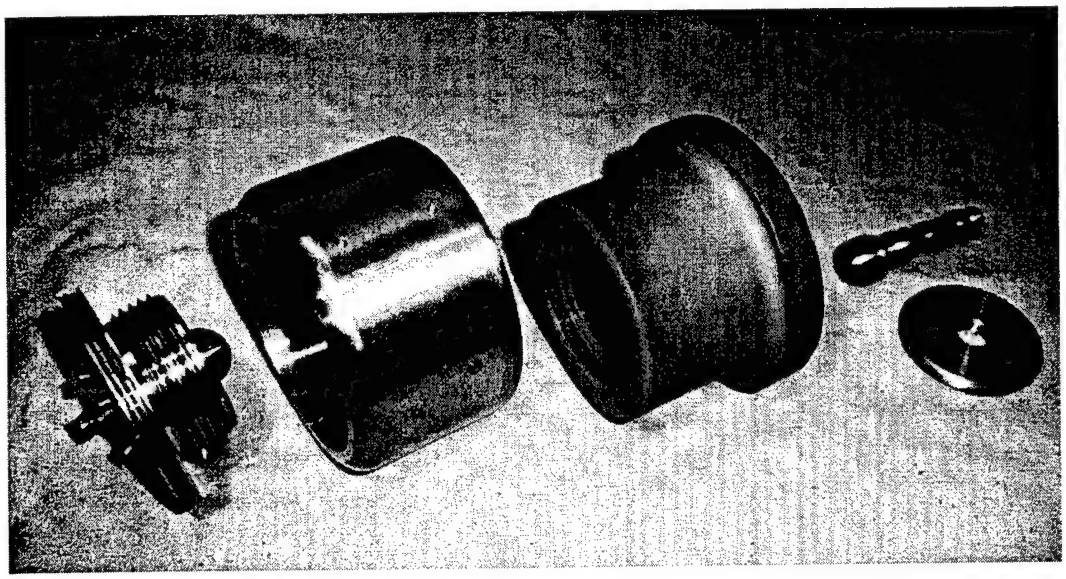

Figure 3.4. Photograph of partially assembled switch.

The electric field profile was computed for the region between the electrodes including the gas flow path around the ferroelectric tip as shown in Figure 3.5. The profile as shown in Figure 3.6 indicates that the electric field is a maximum about 1mm around the gas flow exit tip and relaxes quickly after that. The mechanical design includes a gas flow path to remove gas from the high-voltage electrode side and avoid gas stagnation.

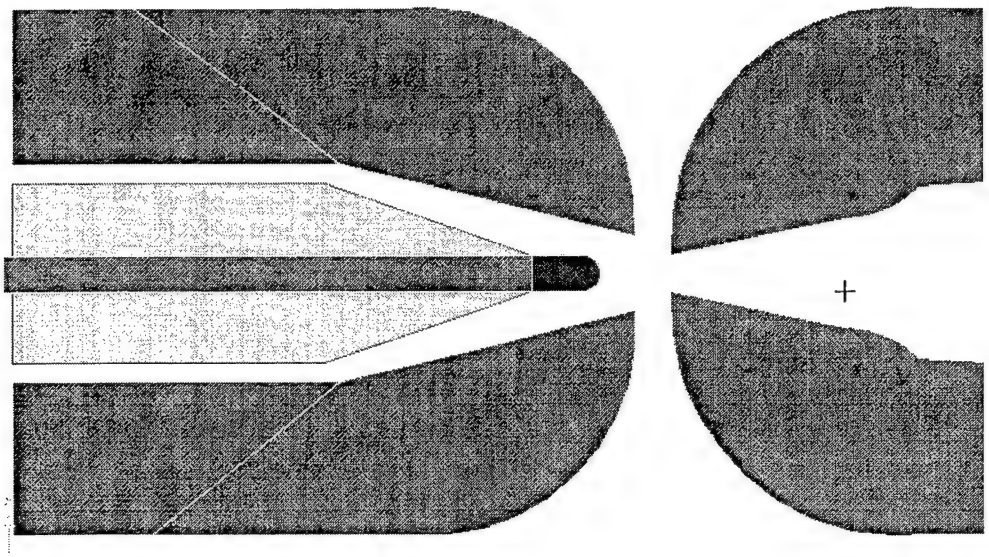

Figure 3.5. Preliminary design of the electrode and trigger set up. The gas flow path is from the back of the grounded electrode (left side) to the high voltage electrode (right side).

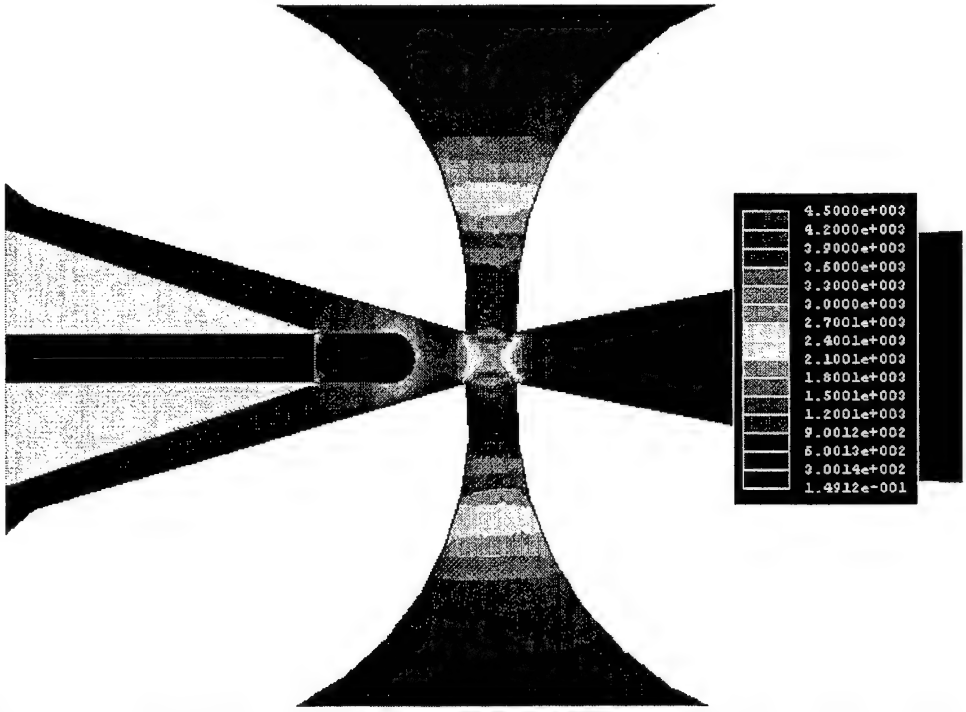

Figure 3.6. Preliminary electric field profile calculation for the switch system.

One of the major features of this design is that the ionized gas moves and fills the region of low field at the center of the electrodes. The field at the edge of the orifice is the nominal high field at which the switch is designed to operate. The ferroelectric tip is not in a high field stress region or in a place where it could arc or come in contact with the external operating voltage of the system.

Gas flow calculations to design the switch are represented in the graph in Figure 3.6. The graph shows the gas flow at the switch gap as a function of input pressure, for a set of input/output cross section areas. The calculations are from Bernoulli's equation. If we assume that we can remain sub-sonic, the actual switch velocity numbers will be smaller.

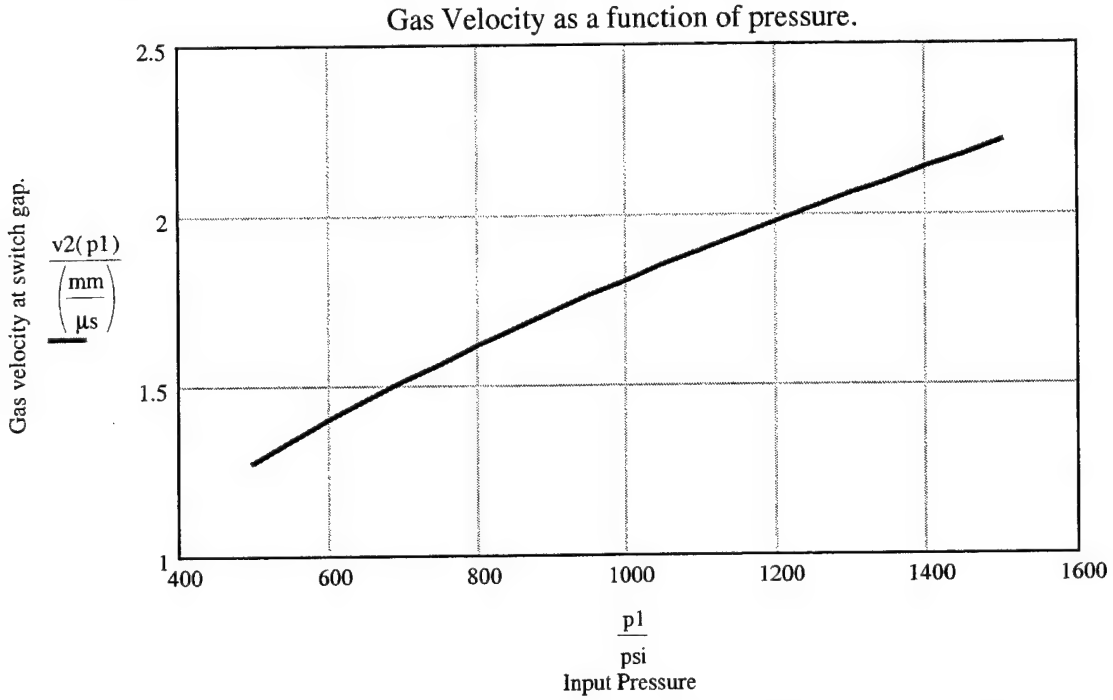

Figure 3.6. Maximum gas velocity vs input gas pressure for a 3:1, input/output, cross section area between electrodes.

IV. Preliminary Results

The pulse used to drive the ferroelectric trigger is provided by a repetition rate circuit built by Ellis Loree. This was originally ordered as a pulse generator with variable output voltage from 200 V to 2 kV, variable rep rate 1 Hz to 1 kHz, output pulse width 1 μs, risetime and falltime of 100 ns. After early experiments, we decided we needed an increased voltage, so a transformer was inserted to boost the voltage to 10 kV. A plot of the final output of the device is shown in Figure 4.1.

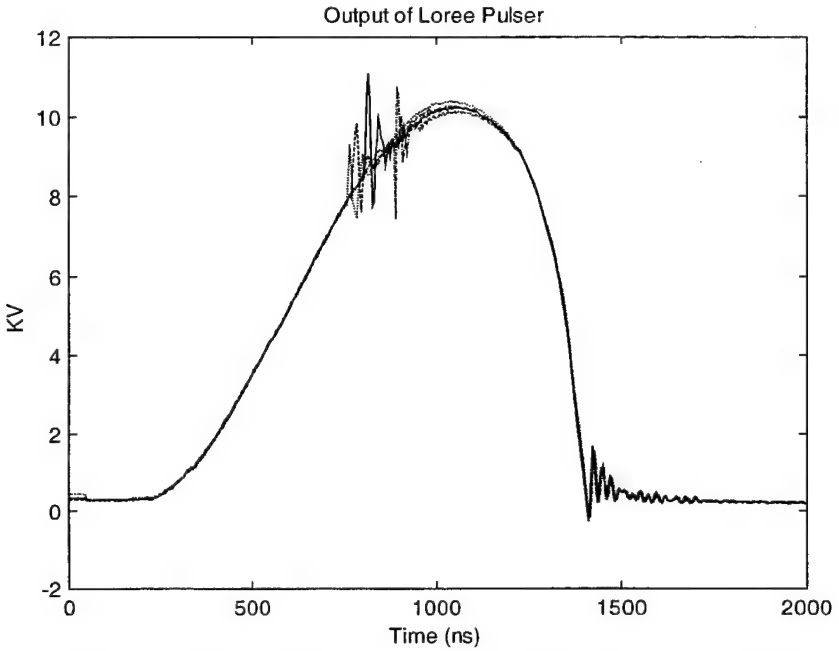

Figure 4.1. Output of high-voltage section of the rep rate circuit, 4 pulses overlaid.

The test setup included a 50 kV DC voltage source and control box, a high-pressure gas regulation and distribution system, and the electrical components associated with the switch. During the preliminary tests described here, the switch setup followed the typical circuit diagram shown in Figure 4.2. C2 is the combination of three TDK capacitors mounted radially on top of the switch. R4 is a 5 kΩ water filled load resistor attached to the side of the switch. A Tektronix CT-1 current probe is mounted below this resistor. The capacitors, load resistor, and CT-1 are shown mounted on the switch in Figure 4.3. An alternate method of examining the output of the switch is the voltage divider made up of R5 and R6. Various resistive voltage dividers were used as voltage sensing probes to measure both the output of the switch and the trigger pulse at the ferroelectric. The trigger pulse at the ferroelectric was normally used to trigger the Tektronix SCD5000 digitizing oscilloscope used to record the data. A laptop computer was used to down load the data from the SCD5000.

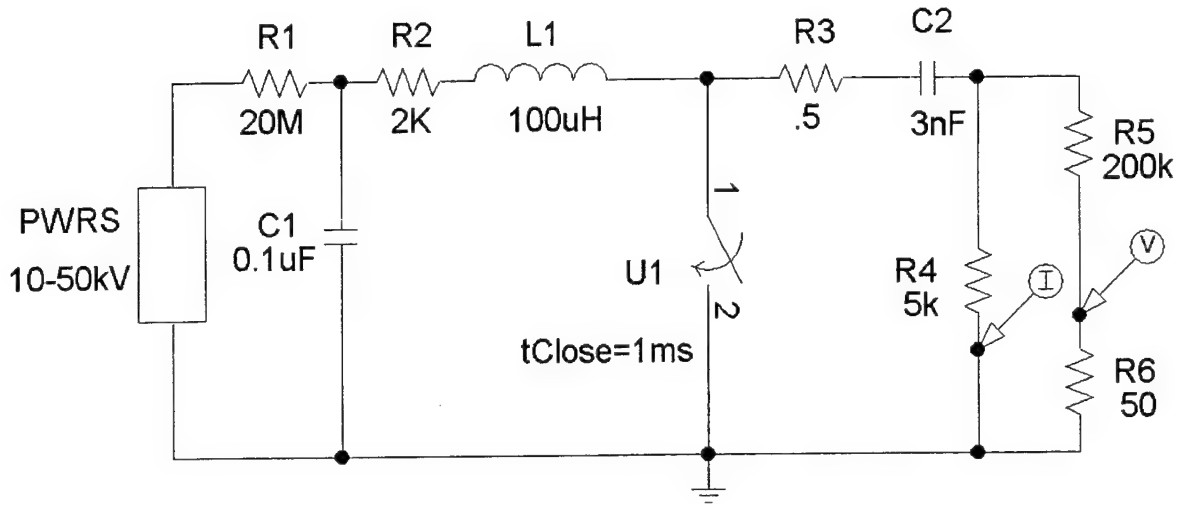

Figure 4.2. Typical test circuit. Current was measured with the CT-1 probe through R4, and voltage was measured across R6. The combination of R2 and L1 is a high-voltage wire-wound resistor with stray inductance. The resistor R3 is a small stray resistance. The capacitor C2 represents the three 1 nF capacitors that are seen on top of the switch in Figure 4.3. The load resistor R4 was made from a tube of soapy water, and is also visible in Figure 4.3. Note that all voltage and current measurements of the switch output were converted to volts across the load resistor, R4.

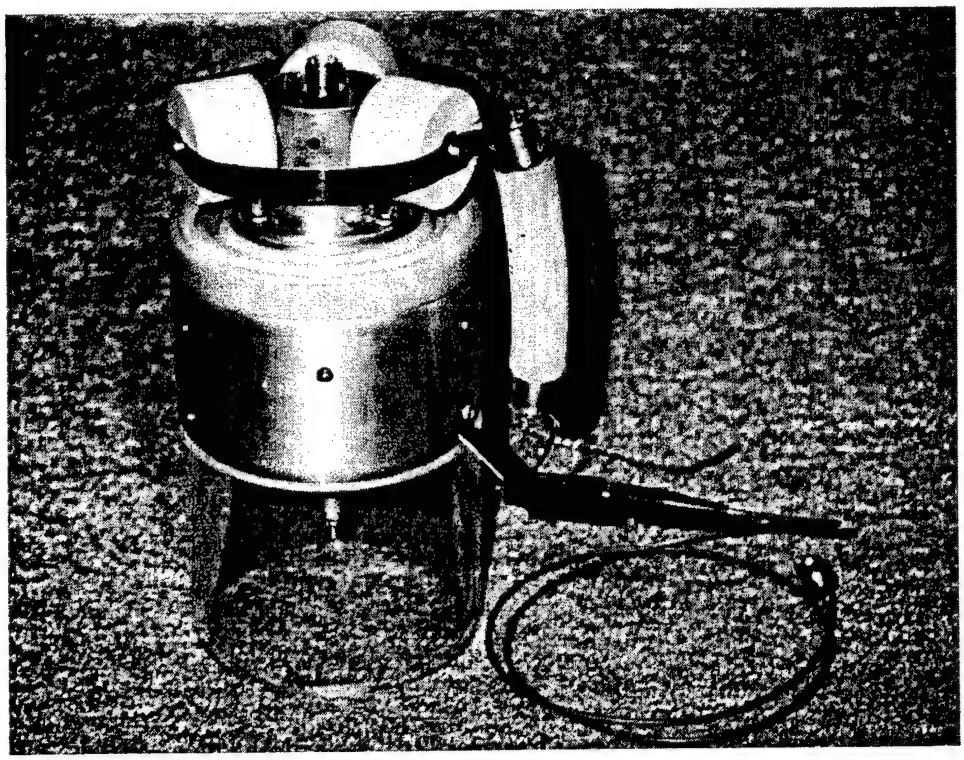

Figure 4.3. Assembled High-Voltage, High-Pressure Switch

The high voltage/high pressure equipment was housed in a Lexan safety box as shown in Figure 4.4. The high-voltage power supply is to the left of the picture. The switch and associated components are located in the right section of the box. A plexiglas stand supports the switch and allows access to the bottom of the switch for the gas and trigger connections. All of the electrical and gas connections are at the rear of the safety box. The SCD5000, laptop computer, and high voltage control box are not shown in this picture.

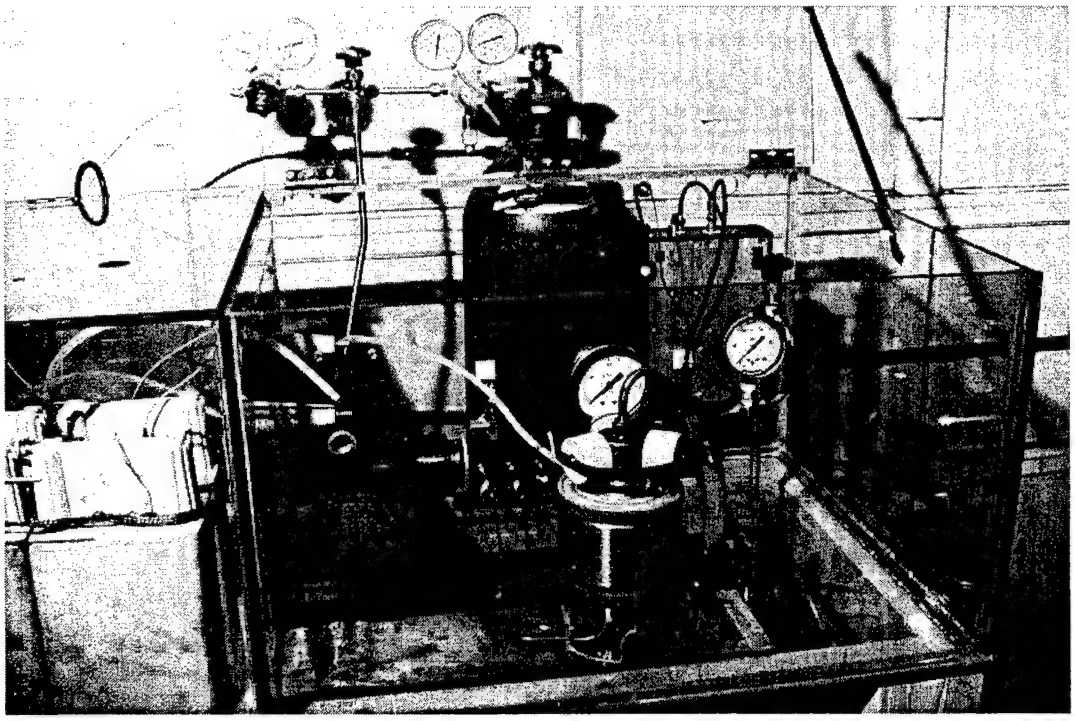

Figure 4.4. Test Setup Inside Lexan Safety Box

Initial testing was carried out using a conventional spark gap with 1 mm spacing, at medium pressure and low gas flow. This was done using a switch of somewhat different design that the one developed here, in order to obtain initial measurements. The rise time at 1 atm is 2.8 ns. Measurements were performed at 0, 10, 20, 30, 40, and 50 psi using dry air. The rise time decreases to about 1.2 ns at 50 psi. To make these measurements, at first we used the voltage divider network to measure the output. Later we used a CT-1 current probe connected to a 5000 Ω water-filled resistor. The CT-1 has a bandwidth of 1 GHz. The voltage across the switch was set high enough so the switch would self-break about once per second. Samples of the data using the CT-1 are shown in Figure 4.5.

There remains some question concerning the validity of our measurements on a very fast time scale. We are attempting to measure risetimes on the order of half a nanosecond, so one would want the circuit elements to all be contained within a volume that is small compared to the risetime length in air—perhaps one-third. In this case with a 500 ps risetime, this suggests that all our circuit elements should be contained within a cube 5 cm on a side. Our load resistor, by itself, is 10 cm long, so we did not meet the criterion. We therefore expect our measured responses will be inaccurate to a degree at early times, but the jitter associated with the switch will be unaffected. So even if our waveform is inaccurate at early times, the low jitter we found is an accurate reflection of the ferratron's characteristics. The solution to this problem is to launch the wave into a TEM structure, and sense the output there. We plan to do so in future work.

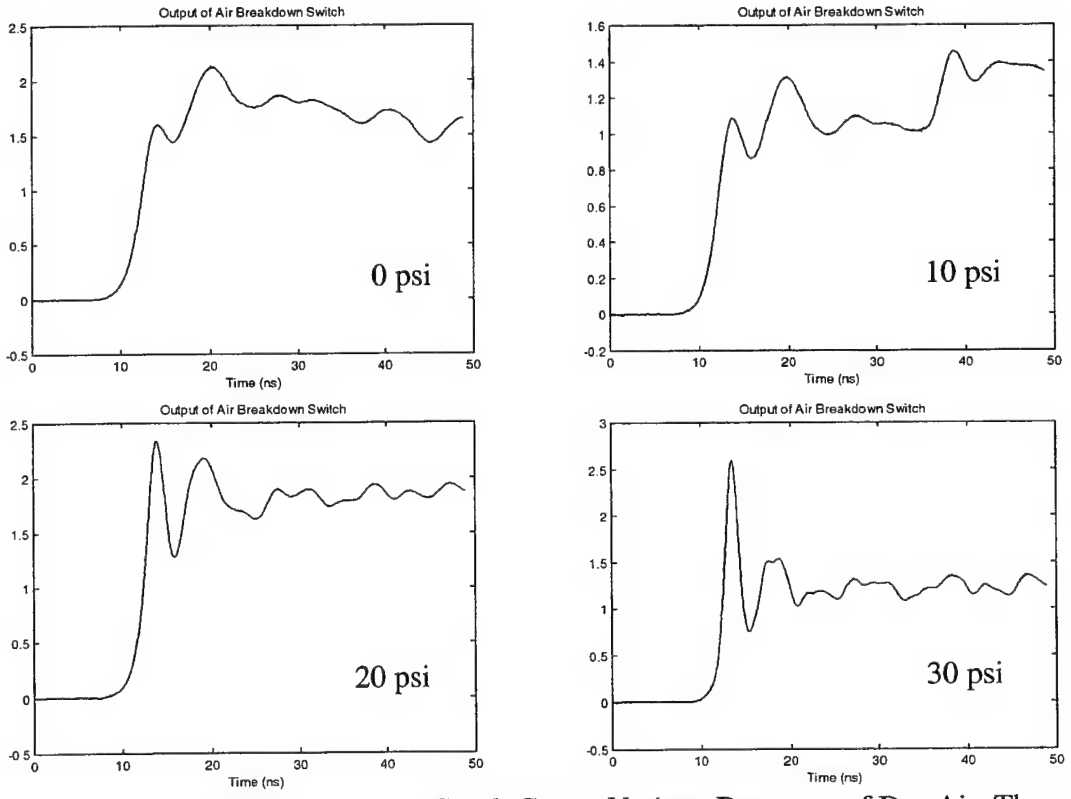

Figure 4.5. Self-Breakdown of a 1 mm Spark Gap at Various Pressures of Dry Air. The vertical scale is kV across R4.

Next, we tested the new ferroelectric switch in self-break mode. The same sequence of measurements was made as with the conventional air switch, except that Nitrogen was used in place of air. Once again, the voltage across the switch was set high enough so the switch would self-break about once per second. Samples of this data also taken with the CT-1 are shown in Figure 4.6. The rise time goes from 1.4 ns down to 1.2 ns.

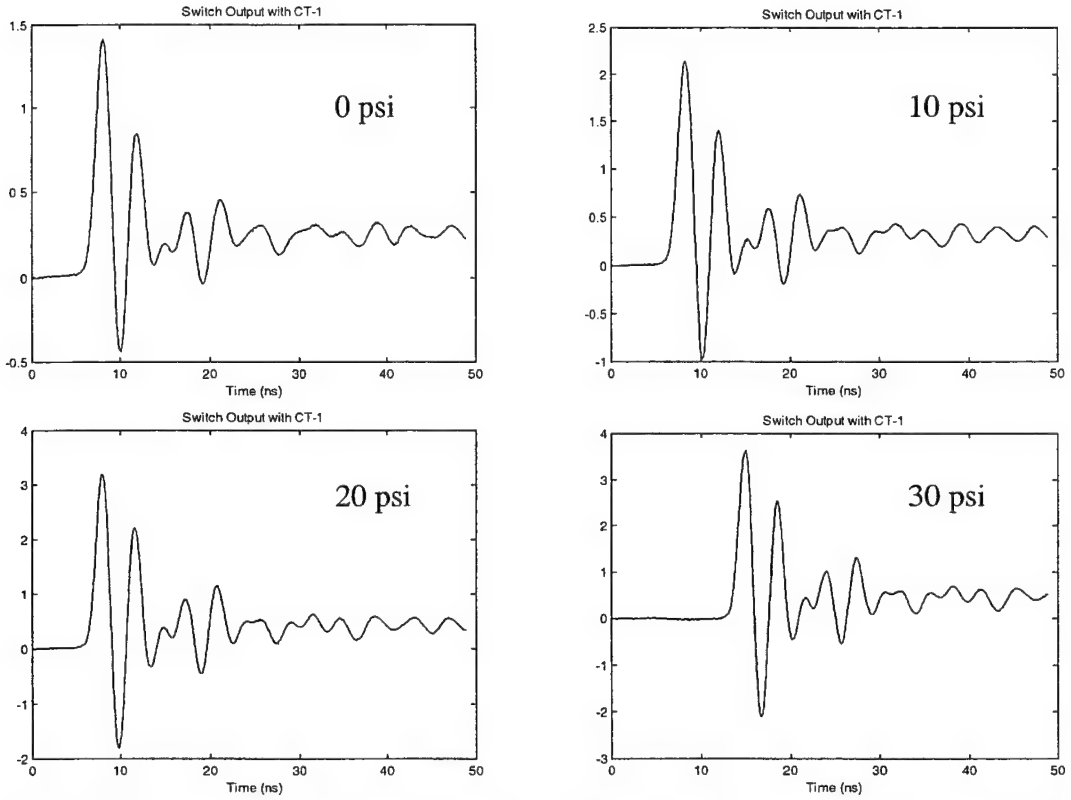

Figure 4.6. Self-Breakdown of a 1 mm Spark Gap at Various Pressures of Nitrogen. The vertical scale is kV across R4.

After testing the switch in self-break mode, data was taken while operating the new switch in trigatron mode, in order to study the jitter due to the switch configuration. The rationale here is that if the jitter is low in trigatron mode, then it will be even lower when triggered by the ferroelectric. To convert the switch to trigatron mode, all it takes is a small change of the configuration at the gap. The trigatron electrode simply replaces the ferroelectric trigger as shown in Figure 4.7. The orientation of the gap was such that there was a positive polarity on the trigatron electrode with respect to adjacent switch electrode (lower). This switch electrode was positive with respect to the other switch electrode (upper).

We measured the output of our switch in trigatron mode on successive shots, and with varying trigger voltages and pressures. The CT-1 current probe was used to measure the current through R4 for these measurements. We overlaid successive shots for each configuration, and the results are shown in Figure 4.8. In most cases, each plot compares 8 consecutive shots out of 16 traces. However, there were a few bad shots that had to be removed.

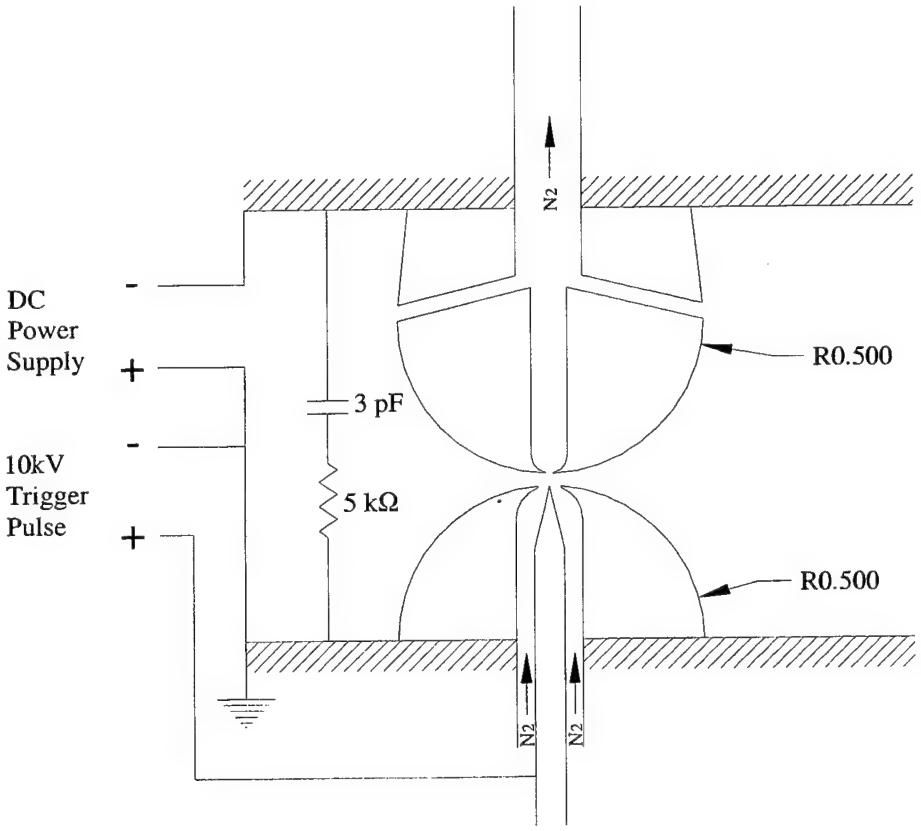

Figure 4.7. Trigatron Switch Configuration.

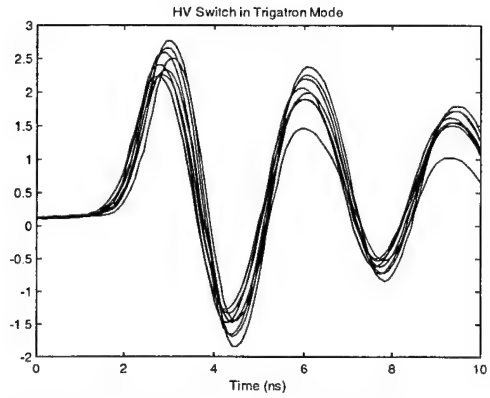

0 psi with approx. 7.5kV input

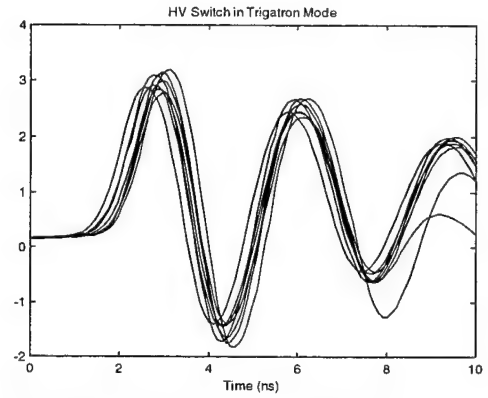

10 psi with approx. 10kV input

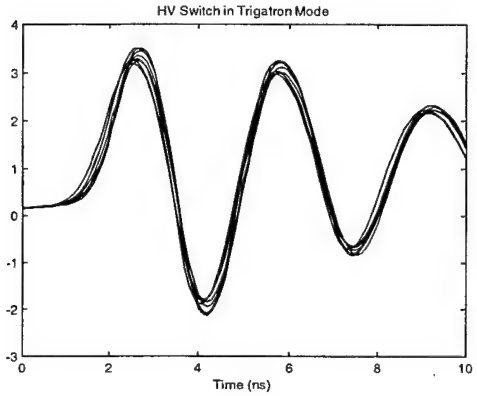

20 psi with approx. 10kV input

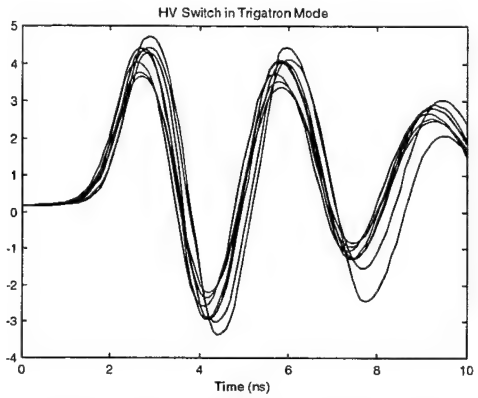

30 psi with approx. 12.5kV input

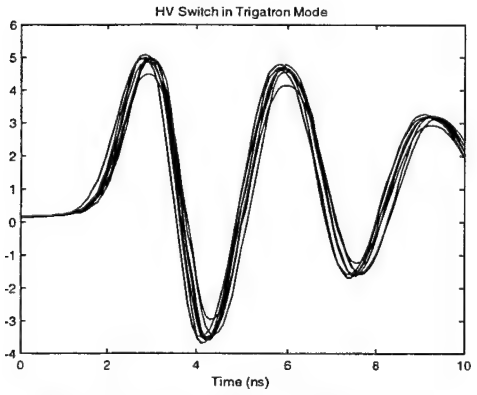

40 psi with approx. 15kV input

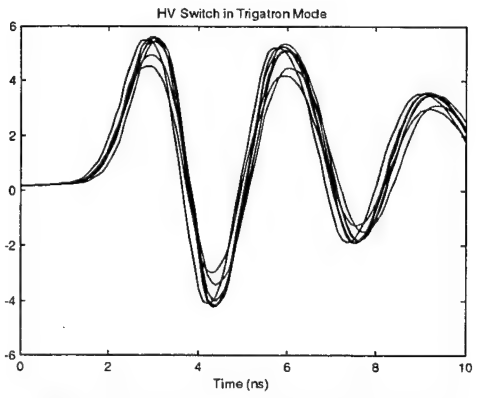

50 psi with approx. 17.5kV input

Figure 4.8. High-Voltage Switch Output in Trigatron Mode. The vertical scale is arbitrary.

The quantity of interest is the line width of the leading edge. For the cases of 20, 30, and 40 kV, the jitter is lowest, and we estimate the line width is about 200 ps. The other cases are worse, and we estimate the line width is about 400 ps with the others. We consider this to be quite reasonable jitter for trigatron mode and we would expect it to decrease when the ferroelectric trigger is used. We provide data below that demonstrates this.

Initially we encountered a number of challenges in implementing the ferroelectric trigger. We believe that the difficulties were the result of using too low a trigger voltage for the particular ceramic being used. The trigger circuit built by Loree was originally designed to be 4 kV, and then was enhanced to 10 kV. Recall that when one uses a voltage that creates a field below the poling field, the electron emission of the ceramic is minimal.

The ferroelectric ceramic triggers used in this switch design (Figure 3.1) are cylinders with inner diameter 0.1 inch and outer diameter 0.185. Both the inner and outer surfaces are silver plated. The trigger pulse is applied between the inner and outer surfaces. For the initial setup, 1 inch ferroelectric cylinders were used with the silver plating on the outer surface partially removed to allow electron emission. Tests were performed with cylinders manufactured with both positive and negative polarizations. By the convention used here, positive polarization means that the poling voltage was positive on the outer surface and negative on the inner surface. Trigger voltages of 4, 10, and 40 kV were used. At 40 kV triggering was noted but after a number of pulses the ferroelectric was damaged.

In order to achieve ferroelectric triggering, the configuration was modified in several ways. First, a 0.5 in long ferroelectric cylinder with negative polarization was used. The silver plating on the outer surface of the cylinder was completely removed. In this configuration, the capacitance between the ferroelectric and the inner wall of the electrode is completes the drive circuit. The diameter of the hole in the electrode is 0.215 in, so the gap between the ferroelectric and the electrode is 0.015 inch. The ferroelectric was positioned about 0.10 in below the surface of the electrode. For the data shown below, the ferroelectric was driven by a positive pulse applied to the inner surface of the cylinder. The gap voltage in the switch was negative on the side with the ferroelectric. Secondly, the 0.1 μF capacitor (C1 in Figure 4.2) was removed from the power supply circuit so that the switch was driven by the 0-50 kV DC power pack through a 20 MΩ resistor. The data shown in Figure 4.9 was taken at 5 - 40 psi with rather high gas flow (not measured). The voltage for each pressure was 9%, 10%, 11%, 14%, 14%, 21%, 23%, 25% of 50 kV as read from the dial of the Variac control. Each plot overlays eight sequential shots taken from sets of 16 traces. The traces were recorded by the SCD5000 at a rep. rate of 1 Hz. A 4000:1 resistive probe connected to the output of the Loree pulser provided the scope trigger. The best jitter occurred at 5 psi in this test and measured about 63 ps. This data is very encouraging even though the rise time is only on the order of 500 ps.

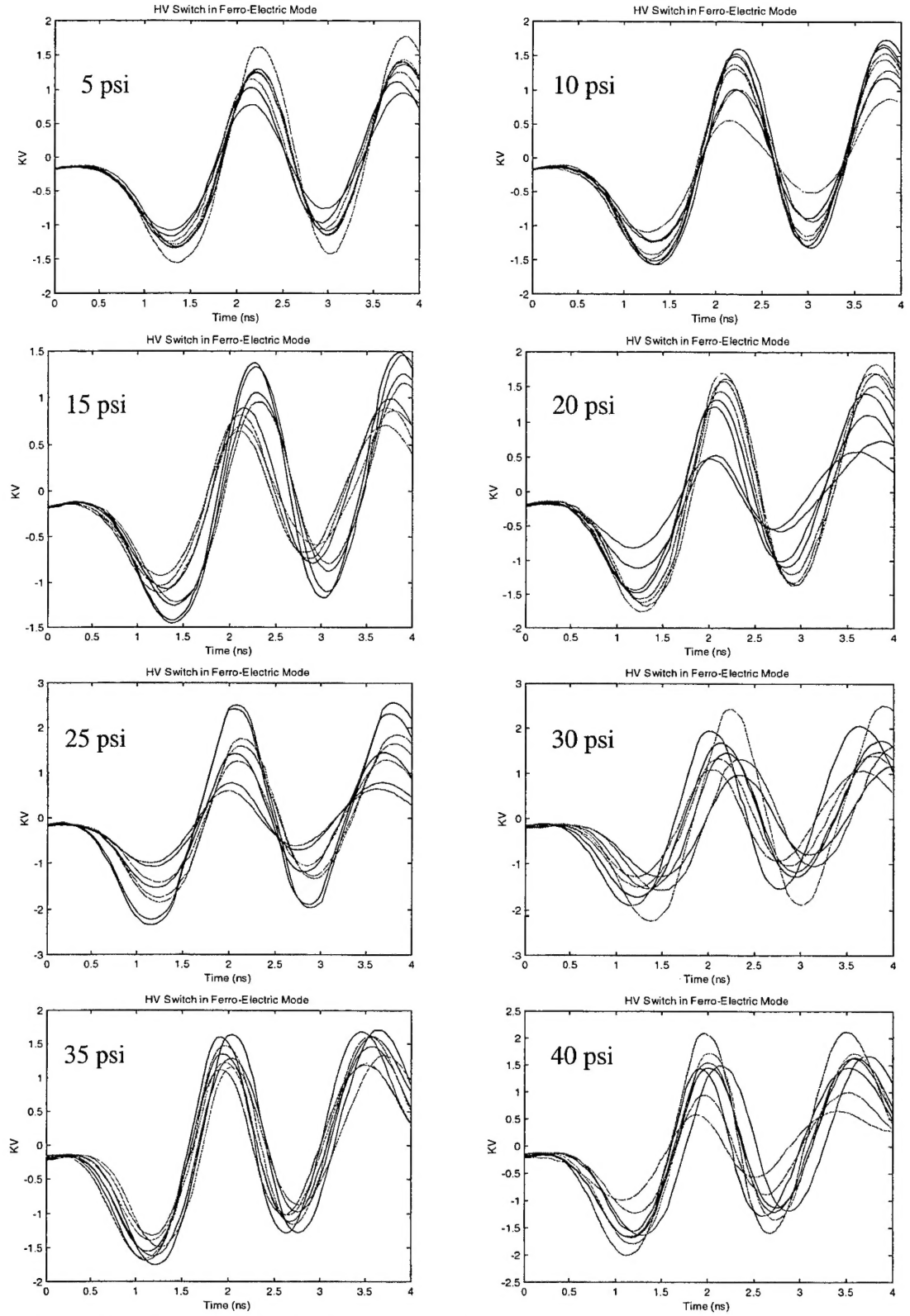

Figure 4.9. Output of High-Voltage Switch in Ferroelectric Mode. The vertical scale is kV across R4.

V. Conclusion

In this note we have introduced the ferratron, which is a high-voltage switch that is triggered by a ferroelectric ceramic. Early measurements of an unoptimized configuration have already demonstrated a functioning ferroelectric triggered switch operating at 2.5 kV, 500 ps risetime, and 63 ps jitter. Additional testing using various configurations of the present switch promises to provide useful information for the development of a low jitter, fast rise time, high-voltage ferroelectric switch.

The ferroelectric materials need to be studied and tested to further characterize the relationships between such parameters as thickness, poling field, pulse width and voltage, and electron emission. Also, the switch design needs to be studied with respect to gap width, operating voltage, gas pressure and flow, and electrode life (erosion rate). The goal of these studies will be to optimize the switch for low jitter, fast rise time, and reliable long life operation.

In future work, we will launch the wave into a TEM structure (TEM horn or coaxial transmission line) in order to avoid the problem of electrically large circuit components.

Patent Notice

A preliminary patent application is pending on the triggered switch described in this note.

References

1. Reitz, J. R., Milford, F. J., and Christy, R. W., Foundations of Electromagnetic Theory, 3rd Ed., Addison-Wesley, 1979, pp. 109-111.
2. Gundel, H., Handereck, J., and Riege, H., Time-Dependent Electron Emission from Ferroelectrics by External Pulsed Electric Fields, *Journal of Applied Physics*,. Vol. 69, No 2, January 15, 1991.
3. Rosenman, G., and Rez, I., Electron Emission from Ferroelectric Materials, *Journal of Applied Physics*, Vol. 73, No. 4, February 15, 1994.
4. Rosocha L. A., Coogan L. L., Secker D. A., and Smith J. D., Applications of Pulsed Power in Oxidation and Reduction Processes for Pollution Control, Ninth IEEE Pulsed Power Conference Albuquerque N.M. 1993.
5. Transducer Products, Route 63 North, Goshen, Conn., 06756.
6. Elizondo, J. M., High Current Cathodes with Controlled A-K Gap Closure, Phase I Final Report, US Army Space and Strategic Defense Command, Contract No. DASG60-93-C-0046, December 21, 1993.
7. O'Dwyer, I., The Theory of Electrical Conduction and Breakdown in Solid Dielectrics, Clarendon, Oxford, 1973.
8. Gundel, H, Riege, H., Wilson, E. G. N., Handereck, J, and Zioutas, K., Fast Polarization Changes in Ferro–electrics and their Application in Accelerators, *Nuclear Instruments and Methods in Physics Research*, A280, 1989.

DISTRIBUTION LIST

AUL/LSE
Bldg 1405 - 600 Chennault Circle
Maxwell AFB, AL 36112-6424 1 cy

DTIC/OCP
8725 John J. Kingman Rd, Suite 0944
Ft Belvoir, VA 22060-6218 2 cys

AFSAA/SAI
1580 Air Force Pentagon
Washington, DC 20330-1580 1 cy

AFRL/PSTL
Kirtland AFB, NM 87117-5776 2 cys

AFRL/PSTP
Kirtland AFB, NM 87117-5776 1 cy

Farr Research
614 Paseo Del Mar NE
Albuquerque, NM 87123 1 cy

Official Record Copy
AFRL/DEHP/Dr Jane Lehr
3550 Aberdeen Avenue SE
Kirtland AFB, NM 87117-5776 5 cy